PRAMANA
— journal of
physics

Vol. 45, No. 3,
September 1995
pp. 291–304

Development of an experimental facility for studying atomic-field, bremsstrahlung from keV electrons interacting with atoms and molecules

S K GOEL, M J SINGH and R SHANKER
Atomic Physics Laboratory, Department of Physics, Banaras Hindu University, Varanasi 221 005, India

MS received 15 May 1995; revised 3 August 1995

Abstract. A dedicated working setup for studying the process of atomic-field bremsstrahlung and its dependence on various parameters for keV electrons incident on a solid or a gaseous target has been indigenously developed. The setup consists of a high vacuum scattering chamber attached with a rotatable X-ray photon detector, a home-built high voltage electron gun with a replaceable tungsten-filament cathode, an isolated floating high voltage system, high vacuum pumping units, various signal processing electronic modules and an IBM PC/XT based 4K-multichannel analyzer. A brief description of the facility is presented. The performance of the facility has been tested by recording the bremsstrahlung spectra from 7·0 keV electrons on thin Ag, Au and 7·5 keV electrons on Hf targets; the corresponding spectra are presented and discussed. The gun can operate in the range of 0–8·0 kV accelerating voltage in the present configuration. Other feasible experiments that can be performed on the setup are also briefly mentioned.

Keywords. Atomic-field bremsstrahlung; electron gun; isolated floating high voltage system.

PACS Nos 34·80; 79·20

1. Introduction

Electron bremsstrahlung (also called, atomic-field bremsstrahlung (AFB)) is commonly understood to be the radiation of a photon in the scattering of an electron from an atom or an ion under its respective screened nuclear Coulomb field. It is one particular consequence of the general coupling of the electromagnetic field and the matter fields. The process is closely related both to elastic electron scattering and to direct radiative recombination in which the incident electron does not scatter but is captured by the atom. Electron bremsstrahlung can teach us about many fundamental aspects of the coupling of radiation and matter fields in addition to an application as a probe for studying the atomic structures.

Electron bremsstrahlung is of immense practical interest and importance for a variety of applications; for example, application in astrophysics (interpretation of astrophysical spectra) and for modelling hot-plasmas, in plasma programmes – both in magnetic confinement and inertial confinement (determination of plasma-temperatures, prediction of plasma properties, estimation of plasma heating). Other applications concern transport and energy-loss of charged particle beams, shielding and radiation damage both to materials and biological tissues. The current understanding of AFB process with major features have been discussed and reviewed by Pratt [1].

Generally, the experimental arrangement for investigating electron bremsstrahlung spectra consists of electron-beam sources, targets, photon detectors and a data

acquisition system. Many experiments have been performed over the years to measure the dependence of the radiation process on a variety of parameters, such as, the incident electron energy, the atomic number of the target material, the photon emission angle and the photon energy. Most of the previous experiments were performed in the high energy range (above 50 keV) of the incident electrons with solid targets [2]. Only recently, experimental data have become available on AFB process in low impact energies with gaseous targets [3].

To study the process of AFB generation, mostly thin solid foils are used as targets however, in some recent experiments, gaseous targets were also employed. In the ideal case, the target should be so thin that the incident electron undergoes only one single collision on the way through it so that the bremsstrahlung process is not disturbed by additional (elastic or inelastic) scattering processes. The advantage in the use of thin targets is that the effect of one single interaction is much easier to calculate theoretically than the corresponding multiple electron scattering problem. Hence, such experiments can be compared much more directly with theory. However, the problems involved in measurements with small counting rates from very thin target foils without destroying them are considerable.

The subject matter of the present paper is concerned mainly with the developmental aspect of an experimental facility for investigating the AFB process as a function of its relevant parameters. Design, fabrication and description of various components of the setup are given. Few typical examples of the recorded spectra of electron bremsstrahlung process are also presented from test runs on the developed facility. The major motivation to develop the said facility for studying the AFB process with solid and gaseous targets originates from three-fold reasons: (i) no such experimental facility is operative anywhere in the country, (ii) there is a great need of experimental data for AFB at keV energies for testing the existing theories and (iii) it is today's demand and concern to develop the indigenous components of the setup in the laboratory itself and to create a culture of designing and fabricating the equipments for use in research and training areas. As a matter of fact, these objectives have invited a challenging task to any researcher in the country. Our effort has been directed to achieve the same within the constraints of our infra-structural facility and funds availability.

2. Design and fabrication of AFB set up

The AFB setup consists of the following major parts:

- a high vacuum scattering chamber
- a high voltage electron gun
- an isolated floating high voltage system
- high vacuum pumping units
- signal processing and data acquisition system

Description of each part is given in the respective subsections as under:

2.1 *High vacuum scattering chamber*

The high vacuum scattering chamber comprises the following components:

(1) main scattering chamber

(2) Faraday cup
(3) target device
(4) rotatable X-ray photon detector

Design and fabrication of each of the above components are described in the following subsections:

2.1.1 *Main scattering chamber*: The high vacuum scattering chamber is a cylindrical stainless steel pipe of 190 mm height and 44 mm inner diameter as shown in figure 1a. It has two collinear ports each fitted with a KF 10 coupling; one adopts a high voltage electron gun and the collimating slits S_1 and S_2 (see, figure 2b), the other couples an insulated Faraday cup (see, subsection 2.1.2). Two slots of height 8·0 mm are cut in the cylinder on both sides of the collinear ports in a horizontal plane containing the electron-beam, the target and the axis of photon detector. Slots are covered with a 6 μ thick hostaphan foil which is strong enough to withstand the pressure in the chamber and transparent enough to transmit the X-ray photons of 2·0 keV energy up to 70%. The top flange of the chamber adopts a movable target holder in the centre which permits the positioning of targets in place without cycling the vacuum of the system.

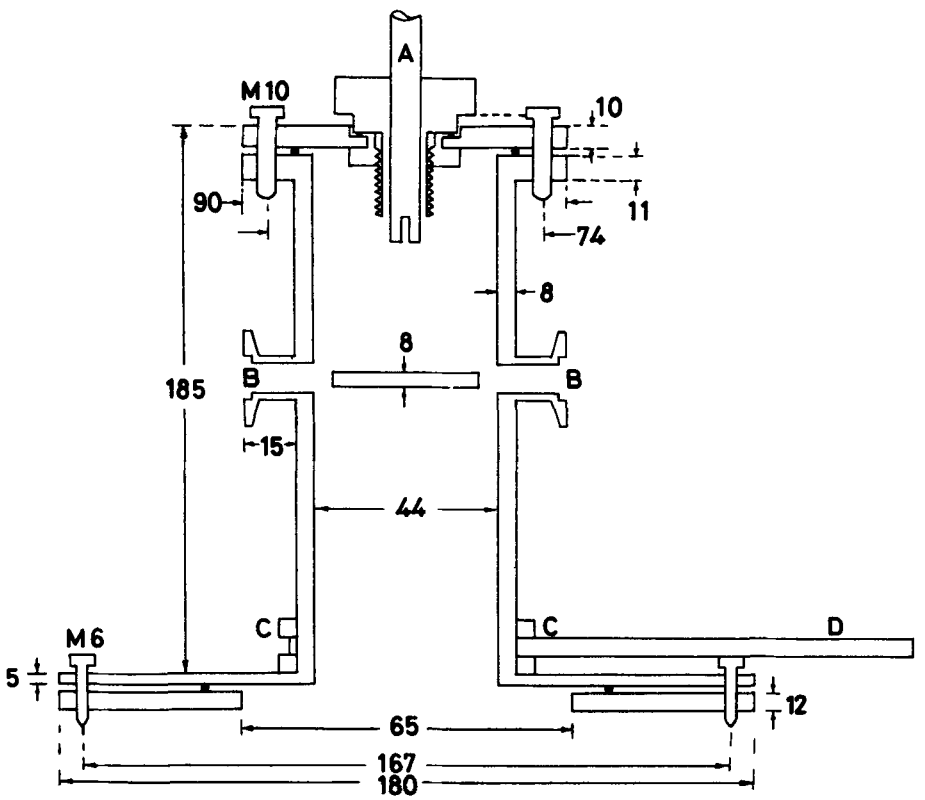

Figure 1a. Cross-section view of the main scattering chamber. A: ϕ 10 mm rotational vacuum feedthrough; B: KF 10; C: SS-collar; D: Al-rotatable platform.

2.1.2 *Faraday cup*: Faraday cup is a device to collect the charge of the transmitted electron beam through the target. In our setup, it consists of two coaxial hollow-Al-cylinders; the length/diameter of the inner and outer cylinders are 25 mm/7 mm and 56 mm/16 mm, respectively. The outer electrode is negatively biased to prevent secondary electrons produced in the inner cylinder from escaping, while the monitoring of the collected charge is made on the latter. The two electrodes are mounted on a perspex flange which has BNC connectors to provide for biasing and current monitoring outputs. The two electrodes mounted on the perspex flange are coupled to an aluminium enclosure (not shown in figure 1b) through a KF 10 coupling at its other end. The current is measured and integrated by a current integrator (ORTEC 439). Figure 1b shows a cross-section view of the Faraday cup with dimensions.

2.1.3 *Target device*: Thin foils of solid targets are mounted on the aluminium frame having 4-consecutive holes each of 12·0 mm diameter. The frame is attached on an insulated SS-shaft which enables the positioning of foils at a desired place and at a chosen angle in the centre of the chamber using a vacuum seal device (see, figure 1c). The gaseous targets are introduced in the collision zone through a tube attached with a hypodermic needle (ϕ 0·5 mm) or with a multicapillary tube with pore size 100 μ (not shown in figure). The effusing gas is finally pumped down by a diffusion pump placed underneath. The adjustment of the input gas pressure in the chamber is done by a fine needle valve (FCV 10 K, L H Alliston, England) in such a way that a single collision condition is maintained. The pressure of the gas in the vicinity of the collision zone is measured by a MKS capacitance manometer (Model 127aa–00001D). The single collision condition is ensured by measuring a linear dependence of the gas pressure as a function of bremsstrahlung photon counts in a chosen energy window (Δk) per incident electron for a given impact energy of the electrons. The target gas pressure measured by the capacitance manometer under this condition has been found to be typically of the order of 3×10^{-3} mbar. The gas density relative to this pressure is estimated to be about 10^{13} atom/cm^3 in the interaction zone. This 'thin' target ensures that multiple scattering events are negligible.

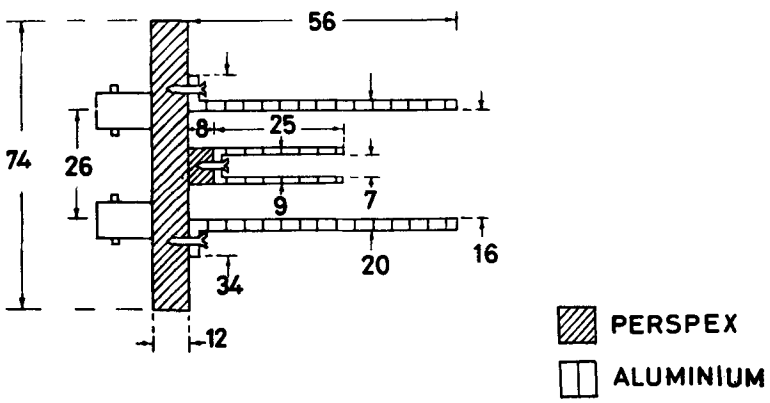

Figure 1b. Cross-section view of the Faraday cup assembly.

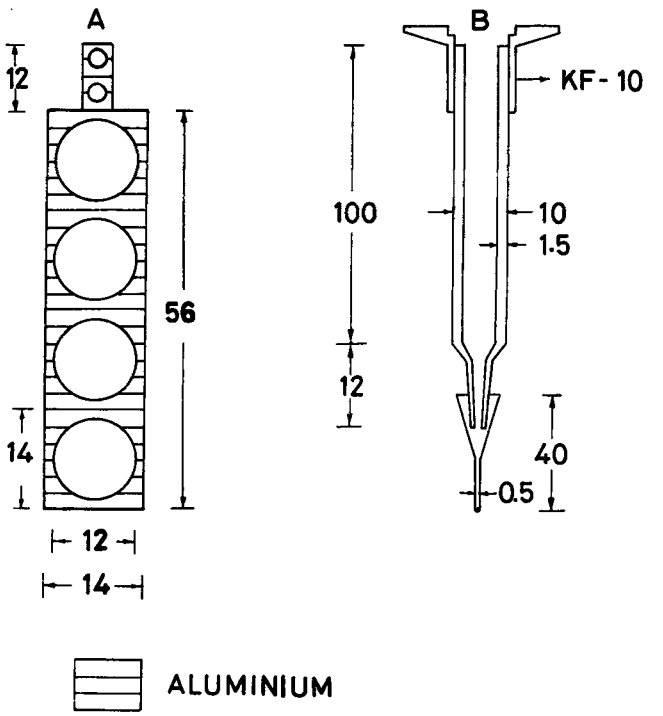

Figure 1c. Solid and gas target devices. A: solid target holder; B: gaseous target device.

2.1.4 *Rotatable Si(Li) X-ray detector*: An aluminium platform (530 mm × 250 mm × 10 mm) is coupled with the main chamber at its one end and rotates about the collision centre (see, D in figure 1a). A Canberra Si(Li) X-ray photon detector (Model SL80175, Cryostat Model 7905–7·5) is placed on this platform with its Be-window facing the 8·0 mm slot. The detector can be positioned at any angle between 30° and 150° on one side and between 210° and 270° on the other side of the collinear ports with a precision of $\pm$ 1°. Alignment of the cryostat with respect to the centre of collision can be made manually on the platform. The bottom of the platform is attached with three metallic supports which rest on the ground. These supports are fitted with an arrangement to adjust their heights as well (not shown in figure 1a).

2.2 *High voltage electron gun*

In the present setup, we have used an electron gun taken out from one of the discarded cathode ray oscilloscopes. Its indirectly heated oxide-coated cathode assembly was removed and it was replaced by an arrangement containing a hair-pin tungsten filament (ϕ 0·15 mm) and a pair of voltage/current feedthroughs as shown in figure 2a. This arrangement with a 'replaceable-filament' is desirable because it allows us to operate the gun with frequent exposures to atmosphere. The tungsten filament is more rugged and resistant to oxidation contrary to the oxide-coated cathodes. The arrangement is made snuggly-fitted to the grid cylinder (G) of the gun (see, figure 2b). The other main

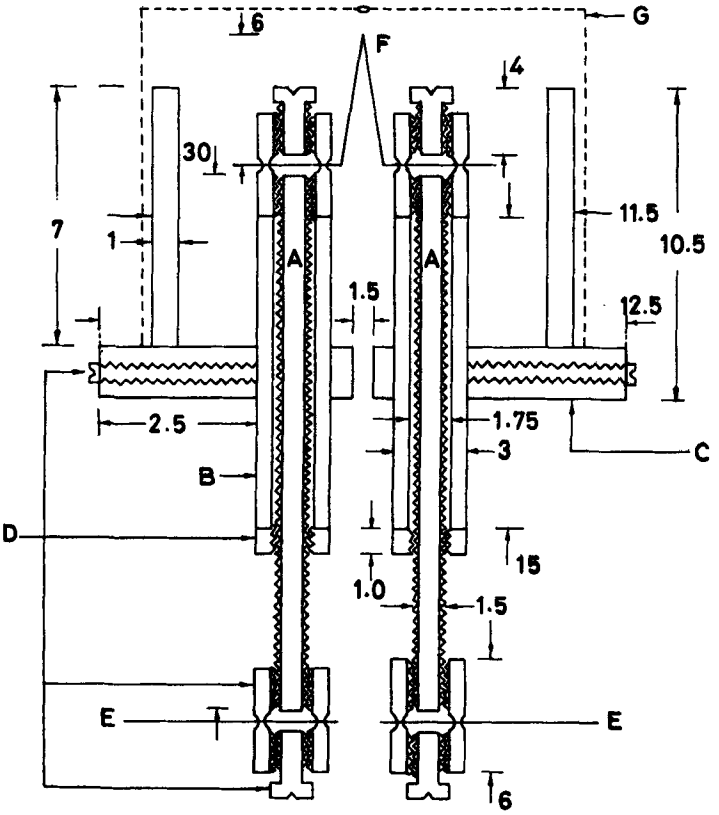

Figure 2a. Cross-section view of the replaceable filament-assembly of the high voltage electron gun. A: copper screw; B: ceramic tubing; C: Al-cylinder; D: Brass nut/bolt; E, E: Filament connecting leads; F: Tungsten filament; G: Grid cylinder.

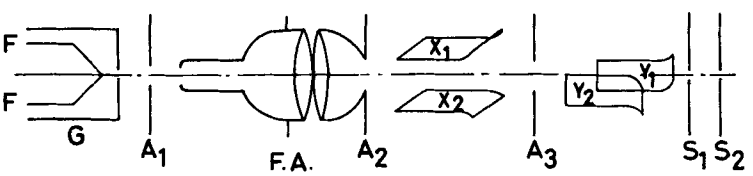

Figure 2b. Schematic sketch of the electron gun with different electrodes. FF: Filament; G: Grid: A_1, A_2, A_3: Anodes; FA: Focussing anode; X_1–X_2, Y_1–Y_2: Deflector plates; S_1, S_2: Collimating slits.

components of the electron gun, namely, control grid, anode, focussing electrode, X- and Y-deflector plates, etc. are shown in figure 2b. The input voltages to each electrode of the gun are provided by pins mounted on a perspex flange having a diameter 100·0 mm and a thickness 12·0 mm. The complete electron gun is made to rest vertically on the perspex flange with three aluminium pillars (ϕ 3·0 mm) attached to the base of the gun. An enclosure for the electron gun has been fabricated out of aluminium which

is coupled with the main scattering chamber through a KF 10 coupling. The other two ports fitted with KF 10 and KF 25 couplings of the enclosure, respectively, provide the facility to connect a Penning gauge and a differential pumping system (VS-114D). A collimating slit assembly S_1 and S_2 having carbon-apertures of 3·0 mm on a copper pipe of length 50·0 mm is fitted between the main scattering chamber and the electron gun enclosure. This arrangement facilitates the alignment of the beam on the target more precisely on one hand and cuts down the background radiation considerably on the other. Various voltages applied to gun-electrodes are discussed in § 2·3.

2.3 *Isolated floating high voltage system*

An isolated floating high voltage system for grid and filament power supplies has been developed. This was necessary in order to keep the anode at earth potential and the cathode/grid at a high negative voltage. A 20 kV isolation transformer (M/s Sairam, Bombay) was used to fulfil this job. Necessary grounding for high voltage and for other units is derived from a common earthing terminal. All units floating on high voltages are enclosed in a cage consisting of 12 mm thick perspex sheets covered with a grounded metallic net. The regulation of voltage/current is made from outside of the cage using the insulator shafts attached to the power supplies. A block diagram showing the electrical connections for the isolated floating high voltage system is given in figure 3.

Two regulated high voltage dc power supplies (0–20 kV, 0–1·5 mA) purchased from M/s FUG GmbH, Germany, were used to provide accelerating and focussing voltages in the gun. The voltage uncertainty of these power supplies is about 1%. The tungsten filament (6 watt) was heated by a constant current power supply (0–15 V, 0–15 A) and the grid voltage was kept slightly negative to the cathode voltage by a separate power supply. A typical set of values for voltage/current on different electrodes for obtaining a well collimated beam (ϕ 3·0 mm) of 6·0 nA on a Ag-target with 6·0 keV electrons is

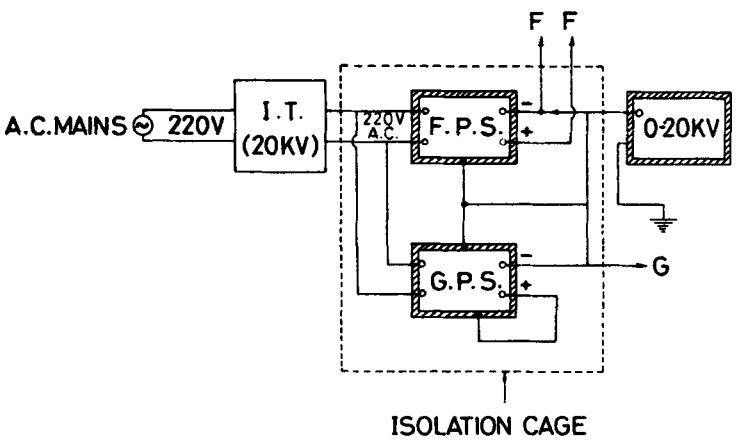

Figure 3. Electrical controls for an isolated floating high voltage system. FPS: Filament power supply; GPS: Grid power supply; IT: Isolation transformer; FF: Leads to filament; G: Lead to grid.

Table 1. Typical values of various voltages and currents applied to gun-electrodes for a beam of 6·0 nA, diameter of 3·0 mm on the target for 6·0 keV electrons incident on a thin Ag foil (157 μgm/cm^2).

Filament voltage	2·1 V
Filament current	3·0 A
Cathode voltage	−6·0 kV
Emission current	0·007 mA
Focussing voltage	−5·92 kV
Emission current	0·000 mA
Grid voltage	−0·5 V
X_1-deflector plate	0·0 V
X_2-deflector plate	100·0 V
Y_1-deflector plate	0·0 V
Y_2-deflector plate	100·0 V
Beam current	6·0 nA

presented in table 1. A visual check of the dimensions of beam spot was made on a ZnS screen placed at the target position.

2.4 *High vacuum pumping system*

The main scattering chamber is evacuated by a 2·5″ oil-diffusion pump (VS-65D, 100 l/s) and the electron gun enclosure by a 4·5″ oil-diffusion pump (VS-114D, 300 l/s); both pumping units are purchased from M/s Hind High Vacuum Co. Pvt. Ltd., Bangalore. The pressures maintained by rotary and diffusion pumps are measured by a Pirani and a Penning gauge respectively. The base pressure attained in the scattering chamber and that in the electron gun enclosure is better than 2×10^{-6} mbar without using a liquid nitrogen trap.

2.5 *Signal processing and data acquisition system*

A block diagram of various electronic modules used for processing the photon and electron signals is shown in figure 4. Standard NIM modules have been used to process the photon signals generated by the Si(Li) detector. A Canberra Si(Li) X-ray photon detector, preamplifier (PA, Model 2008), H.V. power supply (Canberra, Model 30020) and spectroscopy amplifier (Canberra, Model 2020) constitute an integral part of the X-ray photon detection and corresponding signal processing system. An IBM PC/XT based 4K-Multichannel Analyzer (MCA) (M/s Nucleonix, Hyderabad) is interfaced with the photon signals through an ADC (see, figure 4). Data acquisition, stripping and plotting, etc. are carried out on this unit. Monitoring of the beam current is accomplished by a picoammeter (UNIBI, Bielefeld) and integration of which is done by a current integrator (ORTEC 439). All spectra are recorded in the pulse-height analysis (PHA) mode of the MCA and stored in the hard disc/floppy disc of the computer. The spectroscopy amplifier (SA) has a built-in facility to switch the pulse-pile-up rejection on or off while recording the spectra. This provision facilitates the rejection of pulse-pile-up events during acquisition of the data. The shaping time of the SA was chosen to be 12 μs in order to obtain the best resolution of the Si(Li) detector

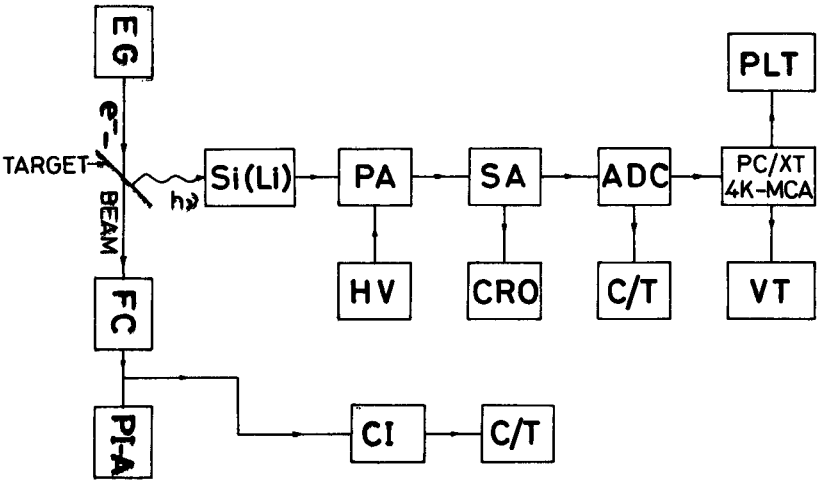

Figure 4. Signal processing and data acquisition system. PA: Preamplifier; SA: Spectroscopy amplifier; ADC: Analog to digital converter; HV: High voltage power supply; CRO: Cathode ray oscilloscope; C/T: Counter timer; VT: Video terminal; PLT: Plotter, CI: Current integrator; PI-A: Pico ammeter; FC: Faraday cup; EG: Electron gun.

(FWHM = 250 eV at 5·9 keV). Emulation software of 4K-MCA is used to accumulate, strip and analyze the data.

3. Operation, test runs and energy calibration

A successful operation of the developed facility essentially involves simultaneous smooth functioning of the vacuum system maintaining the base pressure of the system better than 2×10^{-6} mbar, a stable output of the collimated beam from the electron gun, a photon detector optimized for a high signal to noise-ratio and properly shaped and amplified photon-signals as input to ADC. When all of these are made functional with their optimized values, accumulation of the desired AFB spectra for a chosen target and incident energy is carried out on an IBM PC/XT based MCA in PHA mode (see, figure 4). As AFB intensity depends on Z^2 (Z = atomic number of the target), accumulation time of the AFB spectra depends on the target and beam current used in the experiment. For targets having Z between 40 and 80, data collection times with 1–3 nA beam current are found to be 20–30 minutes more than sufficient for a 2–3% counting statistics. The background radiation arises due to elastic and inelastic scattering of the incident electrons from materials in the neighbourhood of the target used, in particular, the radiation originated in the zone being away from the beam-target interaction region and seen by the detector in a given geometrical configuration contributes maximum. This problem of background radiation can be circumvented by collimating the incident beam with narrow slits and by employing a limited solid angle of the detector. The latter part can be readily achieved by using a narrow aperture on the detector's window. We have investigated the background radiation as a function of

impact energy of the electrons. We found that it increases almost by a factor of two by changing the incident energy of electrons from 2·5 keV to 7·0 keV. However, having considered the above points, one must make note that mere presence of the foreign materials in the vicinity of target can cause background radiation, for example, the materials of the frame on which the targets are mounted are the main source of background radiation. In order to reduce the intensity of the background radiation, it is always preferred to use a low-Z material for constructing the target-frame. Generally, the background radiation is recorded by introducing the empty frame in front of the beam. Nevertheless, this method is good enough as long as there exists a small probability of the incident electrons that are elastically scattered from the target. In AFB spectra, the background subtraction is a serious and important task while analyzing the data for determination of the AFB cross-sections.

A few test runs for AFB spectra produced from 7·0 and 7·5 keV electrons on thin Ag (157 μgm/cm^2), Au (193 μgm/cm^2) and Hf (6·6 mg/cm^2) targets have been carried out on the present facility and displayed in figures 5(a–c) respectively. The spectra have been recorded by placing the photon detector at an angle of 90° and the foil tilted at 45° with respect to the incident beam direction. The channel numbers of the MCA are calibrated for corresponding photon energies by using a standard ^{55}Fe radioactive source. The source is placed at the target position and the characteristic Mn-K_α and K_β

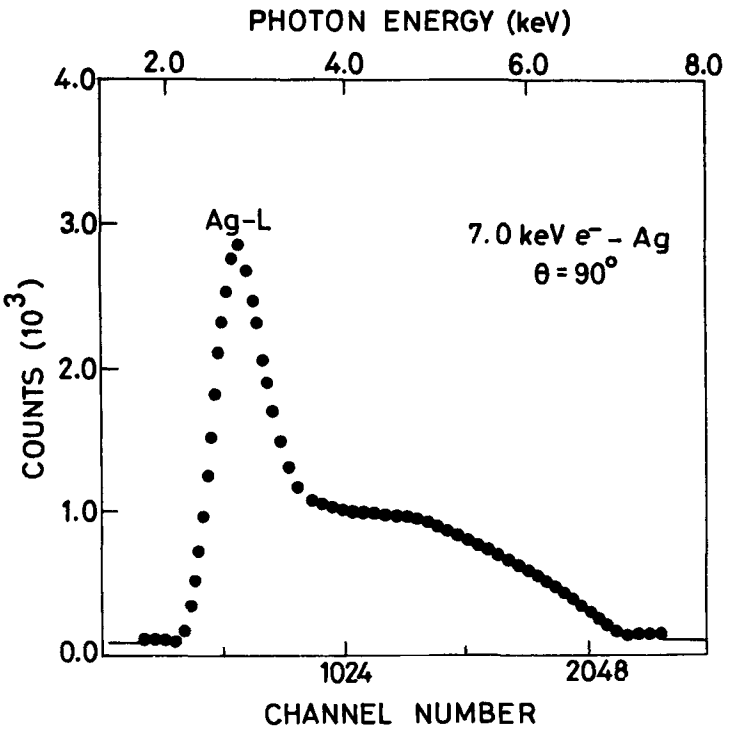

Figure 5a. Electron bremsstrahlung photon energy spectrum for 7·0 keV electrons on a thin Ag target.

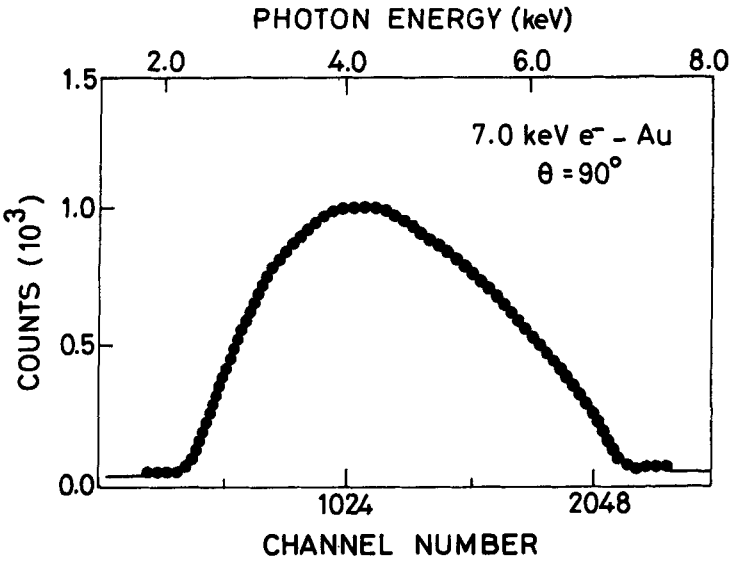

Figure 5b. Electron bremsstrahlung photon energy spectrum for 7·0 keV electrons on a thin Au target.

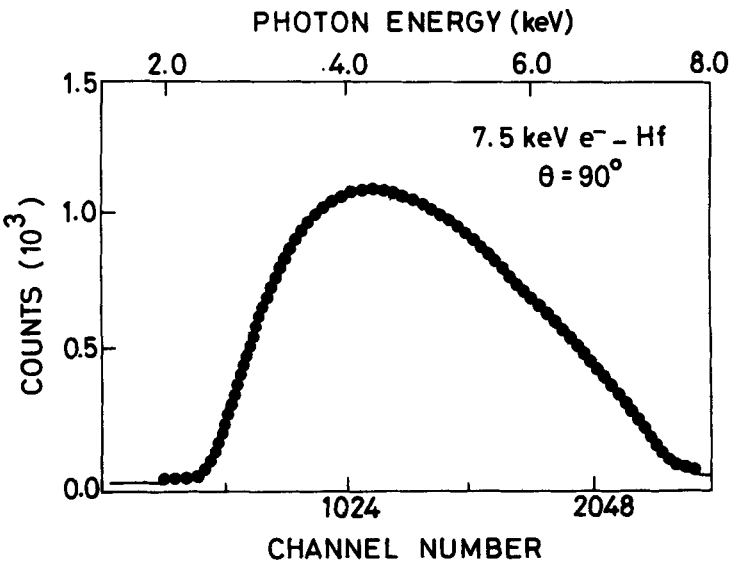

Figure 5c. Electron bremsstrahlung photon energy spectrum for 7·5 keV electrons on a thin Hf target.

lines appearing at 5·9 keV and 6·492 keV respectively are recorded using the identical electronic setup which was employed for accumulating the AFB spectra of different targets. A typical spectrum of ^{55}Fe radioactive source as recorded is shown in figure 6. The relative efficiency of the Si(Li) detector $\varepsilon(k)$ was determined by recording the

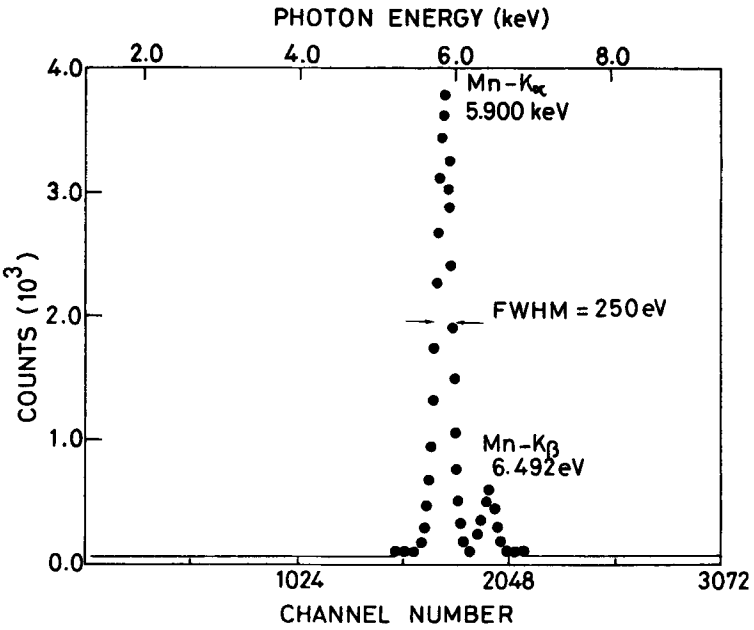

Figure 6. A typical photon energy spectrum from a ^{55}Fe radioactive source.

bremsstrahlung radiation emitted from 7·0 keV e^--Au collision in the photon energy range of 2·0–7·0 keV following the procedure given in ref. [4]. The efficiency was placed on an absolute scale by the measurement of Mn K_α-line from a calibrated ^{55}Fe radioactive source. The corrections for electron back-scattering, energy loss and X-ray absorption were taken into account. The geometrical efficiency of our detector was experimentally determined to be $1{\cdot}71 \times 10^{-4}$ at $k = 5{\cdot}9$ keV while its value from the theoretical AFB cross-section was found to be $1{\cdot}38 \times 10^{-4}$. Both results are found to agree with each other within the uncertainty of the target thickness of 20%. The electron bremsstrahlung spectra produced from gaseous targets are similar and the work in this direction is in progress.

4. Typical results and discussion

Figures 5a–c display the bremsstrahlung photon-energy spectra produced from 7·0 keV and 7·5 keV electrons on thin foils of Ag, Au and Hf respectively. These spectra exhibit a continuous radiation of photons with a well-defined high energy 'tip' appearing at the maximum energy of the incident electrons. In figure 5a, the energy spectrum shows a well-pronounced characteristic Ag-L peak around 3·0 keV over a continuous bremsstrahlung spectrum. Ag-L line could not be resolved into its constituent components due to insufficient resolution of the Si(Li) detector. The cut-off of the low energy photons in all spectra below about 2·0 keV arises due to partial absorption of X-rays in the dead layers of silicon and gold of the detector at Si-K and Au-M edges and partials in the target. Our recent results for the ratio of double

differential cross-sections for the bremsstrahlung photon emission from Ag and Au thin targets when bombarded with 7·0 keV electrons yield an excellent agreement with the theoretical predictions on the relative shape of the spectrum [5].

5. Other feasible experiments with the facility

The present setup as it is and one with some further modification, can be used for other feasible experiments as mentioned below:

1. Angular distribution measurements of the bremsstrahlung spectra as a function of the incident electron energy (T) and the atomic number (Z) of the target.
2. Innershell ionization cross-section of gaseous and solid targets at keV electron energies as a function of Z and T.
3. Measurement of bremsstrahlung photons detected in coincidence with decelerated electrons scattered in a fixed direction; thus information on the elementary radiation process can be obtained and a more stringent test of theoretical work is possible.
4. Multiple ionization of free atoms by using a parallel plate electrostatic analyzer and a time-of-flight spectrometer.

The investigations on problems (3) and (4) above are under active plan which will be taken up in the next phase of the development.

Conclusions

In this work, we have presented the description of a dedicated experimental setup developed indigenously for investigating the atomic-field bremsstrahlung process for keV electrons on a solid or a gaseous target. The design and fabrication of various components of the setup has been given. The high voltage electron gun can operate in the range of 0–8 kV accelerating voltage in the present configuration. The performance of the facility has been tested by recording the electron bremsstrahlung spectra for collisions of 7·0–7·5 keV electrons with thin solid targets and shown that the aimed objectives are fulfilled with satisfaction. It may be mentioned that the estimated cost of our indigenously built high voltage electron gun system is about 5–6 times lesser than that of the custom-built unit. The work with gaseous targets is in progress. Further, other possible experiments on the facility in the area of electron-atom/molecule collisions at keV energies are also mentioned.

Acknowledgements

The work was financially supported by Department of Science and Technology, New Delhi and in part by University Grants Commission, New Delhi. The authors wish to thank all the personnel involved with the fabrication work, specially Shri R M Singh.

References

[1] R H Pratt, *Comm. Atom. Mol. Phys.* **10**, 139 (1981)
R H Pratt, in *Innershell and X-ray Physics of atoms and solids*, edited by D Fabian, H Kleinpoppen and L Watson (Plenum, New York, 1981)

[2] C A Quarles and D B Heroy, *Phys. Rev.* **A24**, 48 (1981) and references therein
[3] M Semaan and C A Quarles, *Phys. Rev.* **A24**, 2280 (1981)
R Hippler, K Saeed, I McGregor and H Kleinpoppen, *Phys. Rev. Lett.* **48**, 1622 (1981)
[4] J Palinkas and B Schlenk, *Nucl. Instrum. Methods.* **169**, 493 (1980)
[5] S K Goel, M J Singh and R Shanker, *Phys. Rev.* **A52** (1995)